OPEN ACCESS
IOP Publishing
Classical and Quantum Gravity
Class. Quantum Grav. **41** (2024) 145009 (19pp)
https://doi.org/10.1088/1361-6382/ad563a

Discovering Love numbers through resonance excitation during extreme mass ratio inspirals

Shani Avitan[1], Ram Brustein[1] and Yotam Sherf[1,2,*]

[1] Department of Physics, Ben-Gurion University, Beer-Sheva 84105, Israel
[2] Max-Planck Institute for Gravitatoinal Physics (Albert Einstein Institute), D-14476 Potsdam, Germany

E-mail: yotam.sherf@aei.mpg.de, ramyb@bgu.ac.il and shavi@post.bgu.ac.il

Received 20 December 2023; revised 22 April 2024
Accepted for publication 10 June 2024
Published 26 June 2024

Abstract

General Relativity predicts that black holes (BHs) do not possess an internal structure and consequently cannot be excited. This leads to a specific prediction about the waveform of gravitational waves (GWs) which they emit during a binary BH inspiral and to the vanishing of their Love numbers. However, if astrophysical BHs do possess an internal structure, their Love numbers would no longer vanish, and they could be excited during an inspiral by the transfer of orbital energy. This would affect the orbital period and lead to an observable imprint on the emitted GWs waveform. The effect is enhanced if one of the binary companions is resonantly excited. We discuss the conditions for resonant excitation of a hypothetical internal structure of BHs and calculate the phase change of the GWs waveform that is induced due to such resonant excitation during intermediate- and extreme-mass-ratio inspirals. We then relate the phase change to the electric quadrupolar Love number of the larger companion, which is resonantly excited by its smaller companion. We discuss the statistical error on measuring the Love number by LISA and show that, because of this phase change, the statistical error is small even for values of the Love number as small as 10^{-4} for moderate values of the spin parameter. Our results indicate that, for extreme-mass-ratio inspirals with moderate spin parameter, the Love number could be detected by LISA with an accuracy which is higher by up to two orders of magnitude than what can be achieved via tidal deformation

* Author to whom any correspondence should be addressed.

effects. Thus, our results indicate that resonant excitation of the central BH during an extreme- or intermediate-mass-ratio inspirals is the most promising effect for putting bounds on, or detecting, non-vanishing tidal Love numbers of BHs.

Keywords: black holes, alternative gravity theories, gravitational waves

1. Introduction

General Relativity predicts that black holes (BHs) do not possess an internal structure. They are 'bald' and can be characterize solely by their mass, angular momentum and charge [1]. Coalescing BHs radiate gravitational waves (GWs) which are being detected by the LIGO and VIRGO observatories since September 2015 [2]. The calculational efforts for improving the accuracy of the general relativity (GR) predictions for the emitted GW waveform, could hopefully provide an opportunity for testing the baldness of BHs. Particularly, the inclusion of tidal interactions may allow us to probe the hypothetical interior structure of the binary companions and quantitatively test the predictions of GR [3–8].

In spite of the increasing precision of ground-based detectors, their limited frequency band enables observations of only a few cycles in the inspiral phase of a binary-BH (BBH) coalescence event for a limited range of masses. The LISA space detector [9, 10], whose design sensitivity is maximal in the mHZ region, is expected to be able to detect and track many BBH coalescence events from the early stages of the inspiral through the merger to the late post-merger ringdown.

In GR, the interior of BHs is vacuum, except for a possibly singular core. But is this their true description? First, a seemingly necessary condition for evading the singularity theorems [11, 12] and the closely related 'Buchdahl-like' bounds [13–16] is that the geometry is sourced by matter that has the maximal negative radial pressure permitted by causality, $p_r = -\rho$, all the way to the surface of the star [17]. Furthermore, if one also considers the emitted Hawking radiation from such a quantum-regularized BH, one finds an untenable violation of energy conservation: When the scale of resolution is parametrically smaller than that of the Schwarzschild radius, the emitted energy of Hawking particles will greatly exceed the original mass of the collapsing matter [18, 19]. Thus, our tentative conclusion is that deviations from GR must extend throughout the object's interior, that is, horizon-scale deviations from GR.

The static quadrupolar Love number k_2 identically vanishes for GR BHs in four spacetime dimensions [20–26], making it a key observable. Measuring non-zero values will indicate a deviation from the GR predictions [27–32]. If indeed horizon scale deviations from the GR predictions occur, then the expectation is that the Love numbers will be small, but not extremely small, suppressed only by some additional perturbative parameter that quantifies the strength of the deviations. The reason for such expectation is that the Love numbers are normalized such that they are order unity if all the dimensional scales are of order of their radius [29, 30].

Previous studies have primarily focused on measuring the Love numbers using tidal deformability, which constitutes a subleading correction to the emitted GW waveform and enters at 5PN order compared to the dominant point-particle term. Tidal-deformability effects are more pronounced at the late inspiral phase. This makes the measurement of the Love number more challenging, since other finite-size effects are also of similar magnitude, requiring the construction of more accurate GW waveforms and detectors with better sensitivity. [3, 33–37].

For GR BHs the inspiral evolution is dominated by the point-particle GW emission. If BHs possess an internal structure, they can be excited. This is reflected by BHs having a spectrum of internal excitations, or internal modes, which can be characterized by their wavelength and

frequency, just as in the case of interior fluid modes of compact relativistic stars. These modes are distinct from the spacetime modes, for example W-modes, which are modes in which the metric is excited as opposed to modes for which the fluid is excited. When the star becomes ultra compact, meaning that the redshift at the horizon is parametrically large, the two branches decouple, and the spacetime modes become very similar to the standard quasinormal modes of the object.

If the orbital frequency becomes comparable to a characteristic frequency of a particular mode, this internal mode can be resonantly excited. This results in a rapid energy transfer from the orbit to the internal mode. The loss of orbital energy effectively advances the inspiral evolution, bringing the companions to a closer and faster orbit. The abrupt energy transfer changes significantly the emitted GW waveform compared to the point particle waveform since it leads to an instantaneous phase jump and a secondary subleading accumulated dephasing due to the differences in orbital velocities. Such resonant energy transfer can only be realized when the BH internal mode is nonrelativistic. By nonrelativistic, we mean modes whose wavelength is comparable to the radius of the compact object $\lambda \sim R$ and whose frequency $\omega \ll c/R$, c being the speed of light. The reason is that the Keplerian orbital frequency is much smaller than the relativistic frequency c/R when the two objects are far from each other, so the orbital frequency and the frequency of the internal mode can be equal only if the frequency of the mode satisfies $\omega \ll c/R$.

Tidal resonant excitations were first discussed in the context of ordinary polytropic stars [38], then, much later, for binaries with at least one of the companions being a neutron star [39–54]. The case in which companion is a generic compact object was discussed in [54–57]. In [58–63], the effect was related to the tidal Love numbers. However, as already mentioned, since the corrections enter the GWs waveform at 5PN order, the effect becomes significant during the late inspiral phase, where additional effects are also significant, making it difficult to detect the Love number with high confidence.

More recent studies related to BH mimickers [64–67], treat the BBH as if they were horizonless ultracompact objects (UCOs). In [64, 66, 67], the tidal field was exciting some additional spacetime modes of a hypothetical spacetime structure outside the UCO. We view these modes as external modes which are distinct from the internal fluid modes, which we discuss. In [67], cavity modes are discussed and derived from solving Teukolsky equations outside a horizonless object. These modes are distinct from the fluid modes that we discuss. In [66], the resulting phase shift due to the resonant excitation of these additional spacetime modes was related to the tidal Love numbers, and the detectability of the quadrupolar Love number k_2 using observations of ground-based GW detectors and the proposed Einstein telescope was discussed. In [65], the detectability prospects of the resonance effects were discussed, but without connecting the effect to the tidal Love numbers. In this study, no evidence for resonance was found in the observations of the first two runs of Advanced LIGO and Advanced Virgo.

Here, in contrast to previous studies, we discuss the tidal excitation of hypothetical nonrelativistic internal modes of the BH, relate the resulting phase shift to the Love numbers and discuss the possible detectability of k_2 in LISA observations of IMRIs and EMRIs. We find that the Love number that can be detected through resonance effects is up to two orders of magnitude smaller than the Love number that can be detected through tidal resonant effects. Thus, we conclude that resonant excitation of the central BH during an extreme- or intermediate-mass-ratio inspirals is the most promising effect for putting bounds on, or detecting, non-vanishing tidal Love numbers of BHs.

We express the model quantities in terms of the dimensionless tidal Love number. We follow the discussion in [29, 66], to relate the resonance phase shift of the excited modes to the

quadrupolar tidal Love number k_2, and their relation to internal modes frequencies of quantum BHs [29–31, 68] and recent frozen star model results [69–71].

We then estimate the statistical error in the measurement of k_2 through resonance excitations during the inspiral of slowly rotating EMRIs and IMRIs, using the design noise spectrum of LISA [9, 72]. We find that the statistical error is small for values of the Love number as small as 10^-4 for intermediate values of the spin parameter. We end with an explicit comparison between the detection prospects of the Love numbers with tidal deformability and tidal resonance, and conclude that resonance excitations are the most promising effect for detecting the Love numbers.

2. Theoretical framework

In the following, we treat the BH as a UCO whose interior is not empty, rather it has an internal structure that supports nonrelativistic fluid modes, similar to relativistic stars. The underlying mechanism providing the pulsation spectrum can be either quantum, for example [73–79], or classical, for example, [69, 70, 80]. In [68], the case was made for UCOs possessing a branch of nonrelativistic internal modes. There, the polymer model [78, 79] of a UCO was discussed. A classical counterpart of the polymer model was later discussed in [69, 70, 80]. A somewhat similar model was also previously discussed in [81] and later in many papers. In [80] it was shown that the frequency of the internal fluid modes is governed by the small parameter $\gamma = 1 - |p_r|/\rho \ll 1$, such that the modes are indeed nonrelativistic $\omega \sim \gamma c/R$.

Making the assumption that the pulsation spectrum does include nonrelativistic fluid modes, we may proceed by using our discussions in [29, 30] about the effect of having such spectrum on the magnitude and sign of the Love numbers, in particular k_2. The discussion is formally similar to the discussions about Love numbers of neutron stars, but the details differ. It follows that once the spectrum is known, we can use the same methods that are used in the standard calculation of Love numbers of neutron stars, irrespective of the origin of the spectrum, be it quantum or classical. For an external observer, the whole interior information can be integrated out to a single quantity—the Love number—which governs the resonance dynamics. Therefore, the parametrization in terms of the Love number employed below, is more general and could apply also to other models of UCOs.

The phase shift result first appeared in [40] in the context of neutron star oscillations, then, much later in [66] in a more relevant context. The purpose of this section is to establish the relevant theoretical framework. So that our novel results, which can be found in sections 3 and 4, could be understood. There, we make the link between the Love number of BH mimickers equations (19) and (20), the resonance phase shift equation (12), and the main result in the detectability section equation (25), which shows how these Love numbers are imprinted in the GW waveform phase.

2.1. Tidal-resonance interaction

Here, we examine the tidal interaction in a binary system, focusing on the central object that is subjected to the weak periodic tidal force exerted by the smaller companion, following the ideas presented in [39, 43, 59, 61] and more recently in [30]. The idea is that the object possesses a set of nonrelativistic fluid modes which are driven by the tidal force and can be therefore described as a collection of driven harmonic oscillators.

The frequencies of the interior fluid modes ω_{nlm}, depend on the radial number n and the angular numbers l, m. We are interested in the dominant effect which is due to the excitation of

the fundamental $n=1$ mode by the quadrupolar tidal field, so we focus on the case $l=m=2$ [43]. As for the other modes; the spherically symmetric static $m=0$ mode cannot generate pressure gradients that are needed for resonance excitation and therefore is not relevant to our discussion. The $m=1$ mode can be resonantly excited in the case that the spin-orbit configuration is misaligned [43, 45]. Here, we restrict our attention to spin vectors that are aligned with the orbital angular momentum and assume that $\omega_{122} \ll c/R$.

When the frequency of one of the interior modes of the central, larger, object, matches the orbital frequency of the companion, it is resonantly excited and efficiently absorbs energy from the orbital motion. The instantaneous energy absorption increases the orbital velocity and shortens the inspiral duration, thus leading to a phase difference in the emitted GW waveform, when compared to the emitted waveform in the absence of a resonance. To calculate the dephasing of the GW waveform, we adopt the derivation in [40, 44], resulting in the following phase evolution,

$$\begin{cases} \Phi(t) = \Phi_{\rm PP}(t) & t < t_{\rm R} \\ \Phi(t) = \Phi_{\rm PP}(t+\Delta t) - \Delta\Phi & t > t_{\rm R} + \Delta t, \end{cases} \tag{1}$$

where $\Phi_{\rm PP}(t)$ is the point particle phase, $t_{\rm R}$ is the time at which the resonance starts, Δt is the resonance duration and $\Delta\Phi$ is the instantaneous resonance phase difference, which in general depends on the object's properties as demonstrated below. The point particle phase $\Phi_{\rm PP}$, is independent, by definition, on the object's composition. In particular, it has the same value for a GR BH and one endowed with an internal excitation spectrum, such as the objects we are discussing.

The number of orbits at resonance scales as [40, 44]. The resonance time scales as $\Delta T_{\rm res} \sim \sqrt{t_{\rm rr} t_{\rm orb}}$. For small mass ratios, $t_{\rm rr}^{-1} \sim q M_1^{5/3} \omega^{8/3}$ is the gravitational radiation reaction time scale that governs the mode time evolution and $t_{\rm orb} \sim \Omega^{-1} \simeq \omega^{-1}$ is the orbital period that characterizes the typical resonance lifetime. The result is that $\Delta T_{\rm res} \sim 1/\sqrt{(q)} t_{\rm orb}$. For $q \sim 10^{-3} - 10^{-4}$ with frequencies $f = 10^{-2} - 10^{-3}$Hz, the resonance time scale $\Delta T_{\rm res} \sim N/f \sim 10^4 - 10^5sec\sim$ 0.1-1 days. It follows that $\Delta T_{\rm res}$ is short compared to the duration of the inspiral, as typical inspirals last from months to years. Assuming that the resonance duration is short compared to the inspiral duration and under adiabatic evolution, we arrive at the frequency domain resonance phase [40, 44],

$$\Phi(f) = \Phi(f)_{\rm PP} + \Theta(f - f_{\rm R}) \left(\frac{f}{f_{\rm R}} - 1 \right) \Delta\Phi_{\rm Res} \,, \tag{2}$$

where $f_{\rm R}$ is the internal mode frequency which satisfies the resonance condition $2\pi f_{\rm R} = m\Omega$, Ω being the orbital angular velocity. Resonance corrections to the phase $\Delta\Phi_{\rm Res}$, are composed of two terms; a dominant term that enters at 2.5PN order higher than the leading order point-particle term and a subleading 4PN-higher contribution. The dominant contribution, which is frequency independent and proportional to $\Delta\Phi$, originates from the instantaneous energy absorption during resonance. The subleading term, which is proportional to the frequency, is a secular effect that increases towards the late stages of the inspiral.

2.2. The phase shift

Fluid perturbations of compact objects are described by the displacement vector ξ^i, of a fluid element from its unperturbed position, which is given by the orthonormal basis decomposition,

$$\xi^i = \sum_n a_n \xi^i_n, \tag{3}$$

ξ_n being the normal displacement vectors, and a_n are the dimensionless displacement amplitudes[3]. In the presence of tidal forces, the fluid modes satisfy the damped-driven harmonic oscillator equation [39, 45],

$$\ddot{a}_{nlm} + 2\gamma_n \dot{a}_{nlm} + \omega_n^2 a_{nlm} = \mathcal{F}(t)_{nlm}, \tag{4}$$

where $\gamma_n = -\mathrm{Im}\,\omega_n$ is the damping rate of the mode. The source of the damping and its precise magnitude are irrelevant for the resulting resonant excitation and dephasing. So, γ can be neglected altogether (see below equation (12) and appendix).

The external periodic force $\mathcal{F}(t)_{nlm}$ excites the nth mode interior fluid mode is given by

$$\mathcal{F}(t)_{nlm} = N_{lm} \frac{\mathcal{E}_l Q_{nl}}{MR^2} \mathrm{e}^{-\mathrm{i}m\phi(t)}\ , \tag{5}$$

where M and R are the mass and radius of the central object. The order unity factor N_{lm} is proportional to the Wigner function and is specified below. The tidal field of the l mode is denoted by $\mathcal{E}_l$, which for the $l=2, m=\pm 2$ satisfies $\mathcal{E}_{ij}x^i x^j = \mathcal{E} r^2 Y_{2\pm 2}$. The mass moment of the quadrupolar nth mode Q_n is given by the overlap integral [40],

$$Q_n = -\int \mathrm{d}^3 r \delta\rho_n r^2\ , \tag{6}$$

where $\delta\rho_n$ is the corresponding energy density perturbation.

Next, we aim to find the instantaneous phase shift $\Delta\Phi$ and the corresponding phase evolution in equation (1). We start by solving equation (4) for the amplitudes a_n, which at resonance is given by [45],

$$a_n(t) = \left(\frac{\pi}{m\ddot{\phi}}\right)^{1/2} \frac{\mathcal{F}(t)_{nlm}}{\gamma_{nl} - i\omega_{nl}} \mathrm{e}^{-\mathrm{i}\omega_{nl}t}, \tag{7}$$

where $\ddot{\phi}$ denotes the rate of change of the orbital frequency at resonance. The transferred energy to the mode nlm during the resonance is a sum of kinetic and potential terms [39, 45],

$$E_{nlm}(t) = \left(\frac{1}{2}\dot{a}_{nlm}(t)^2 + \frac{1}{2}\omega_{nl}^2 a_{nlm}^2(t)\right) MR^2\ . \tag{8}$$

The total energy absorbed by the mode, neglecting γ_{nl}, is given by

$$\Delta E_{nlm} = N_{lm}^2 \frac{\pi}{4m\ddot{\phi}} \frac{(\mathcal{E}_l Q_{nl})^2}{MR^2}\ , \tag{9}$$

[3] We use relativistic units $G, c = 1$.

where $\mathcal{N}_{nlm}$ is the numerical factor we get when writing the spherical harmonics in STF tensor base and is given by [82]

$$\mathcal{N}_{lm} = \frac{(-1)^l 2^{m-1}}{\Gamma\left(\frac{-l-m+1}{2}\right)\Gamma\left(\frac{l-m}{2}+1\right)}\sqrt{\frac{8\pi\,(2l-1)!!}{2l!}\frac{\Gamma\,(l-m+1)}{\Gamma\,(l+m+1)}}. \tag{10}$$

The resonance excitations lead to a phase shift, since the orbital energy decreases as it excites the interior modes. Accordingly, the orbital velocity increases and the inspiral duration decreases by a time Δt. To estimate Δt, we follow [44]. The energy absorbed by the central objects decreases the energy of the orbit by the same amount. In the absence of resonance, such a decrease in energy can only occur by the emission of GW and the time that it would take the orbit to emit GW with such energy Δt would be determined by the equality $\dot{E}_{\rm GW}\Delta t = \Delta E_{nlm}$. The rate of GW emission $\dot{E}_{\rm GW}$ is, to a very good approximation, the same rate as in the absence of resonance, which to leading order is given by $\dot{E}_{\rm GW} = \frac{32}{5}(\mathcal{M}_c\,\Omega)^{10/3}$, with $\mathcal{M}_c$ being the chirp mass. The resulting phase shift $\Delta\Phi = m\Omega\Delta t$ is the following,

$$\Delta\Phi_{nlm} = m\Omega\frac{\Delta E_{nlm}}{\dot{E}_{\rm GW}} = \frac{5}{32}\,m\Omega\,\frac{\Delta E_{nlm}}{(\mathcal{M}_c\,\Omega)^{10/3}}. \tag{11}$$

For IMRIs or EMRIs $\mathcal{M}_c \approx Mq^{3/5}$ and $\dot{E}_{\rm GW} \sim v^{10}$.

Using equation (9), we may calculate the phase shift induced by the leading order quadrupolar mode $l = m = 2$ [40, 66],

$$\Delta\Phi_{n22} = \frac{25\pi}{1024q\,(1+q)}\frac{1}{R_1^5}\frac{|Q_{n2}|^2}{M_1\omega_{22}^2R_1^2} = \frac{25\pi}{2048q\,(1+q)}\frac{1}{R_1^5}\frac{|Q_{n2}|^2}{\Delta E^{\rm int}}, \tag{12}$$

where we used that $N_{22} = \sqrt{3/32}$. Here $q = M_2/M_1$ is the mass ratio and $\Delta E^{\rm int} = \frac{1}{2}M_1\omega_{22}^2R_1^2$ is the internal energy of oscillations which is related to the energy stored in the nth mode by $\Delta E^{\rm int} = \sum_n \Delta E_{n22}$, [59].

We wish to justify our estimate of Δt using only $\dot{E}_{\rm GW}$ and neglecting other dissipation effects. In general, the time difference Δt should include all types of dissipation channels, mainly the dominant dissipation due to tidal friction and the subleading tidal deformation. However, the rate of work of tidal friction is given by [83, 84] $\dot{E}_{\rm TF} = \frac{1}{2}Q_{ij}\dot{\mathcal{E}}^{ij} \sim k_2 v^{15}\nu/M$, where ν is the kinematic viscosity giving rise to viscous dissipation. In [84], it is demonstrated that, under reasonable assumptions, the contribution of viscous dissipation is negligibly small compared to the leading order GW emission and, therefore, can be ignored. For example, for cold neutron stars, considered to be highly viscous $\nu/M \approx 10^{-7}$, whereas for BHs $\nu/M = 1$ [85]. During the inspiral, when the orbital velocity is nonrelativistic the ratio of the different emission rates scales as $\dot{E}_{\rm TF}/\dot{E}_{\rm GW} \sim v^5 \ll 1$, which shows that the internal dissipation effects can indeed be neglected.

3. Fluid-origin Love numbers

Here we follow [29, 30] to determine the relationship between the Love number and the spectrum of internal fluid modes. We focus on the static tidal Love number, ignoring dissipative effects.

Following [30] (see also [39, 43, 59, 61]), we wish to find the static response of the object to an external tidal field. At low frequencies, away from resonance, the amplitude in equation (7) reduces to

$$a_n = \frac{\mathcal{E} Q_n}{M\omega_n^2 R^2} \ . \tag{13}$$

Then, we apply the normal mode decomposition identities $Q = \sum_n a_n Q_n$, and $\delta\rho = \sum_n a_n \delta\rho_n$, and relate the asymptotic moment to the overlap integral equation (6)

$$Q = -\sum_n a_n \int \mathrm{d}^3 r \delta\rho_n r^2 = -\int \mathrm{d}^3 r \delta\rho r^2 \ . \tag{14}$$

Accordingly, using equation (13), the asymptotic moment can be written by

$$Q = \sum_n \frac{Q_n^2}{M\omega_n^2 R^2}\mathcal{E} \ . \tag{15}$$

Then, from the definition of the Love number, $Q = \frac{2}{3}k_2 R^5 \mathcal{E}$, we obtain

$$k_2 = \sum_n \frac{3}{2R^5}\frac{Q_n^2}{M\omega_n^2 R^2} \ . \tag{16}$$

We now approximate k_2 by the first term in the sum in equation (16) relying on a physically motivated assumption. The sum in equation (16) is dominated by the fundamental $n = 1$ mode. The justification is that the number of nodes in the overlap integral in equation (6) increases as n increases. It follows that the contribution of Q_n decreases as n increases. Using the $l = 2$-mode excitation energy $\Delta E_n^{\rm int} = \frac{1}{2}M\omega_{n2}^2 R^2$, the sum in equation (16) can be approximated as

$$k_2 \ \simeq \ \frac{3}{4R^5}\frac{Q_1^2}{\Delta E_1^{\rm int}} \ . \tag{17}$$

We now observe that a similar expression to the one in equation (17), appears in equation (12) which determines the phase shift $\Delta\Phi_{122}$. This allows to express $\Delta\Phi_{122}$ in terms of k_2,

$$\Delta\Phi_{\rm Res} = \frac{25\pi}{1536}\frac{k_2}{q(1+q)} \ . \tag{18}$$

We are interested in the case of small mass ratios, $q \lesssim 1/1000$ and a small but not extremely small k_2, $k_2 \lesssim 1/10$. Then we can parameterize the resonance dephasing by

$$\Delta\Phi_{\rm Res} \ \simeq \ 5 \times \left(\frac{k_2}{10^{-1}}\right)\left(\frac{q}{10^{-3}}\right)^{-1} \ . \tag{19}$$

The resonance-induced dephasing is governed by the dimensionless tidal Love number and the companion's mass ratio. Generally, the detection threshold for the instantaneous phase jump requires $\Delta\Phi_{\rm Res} \gtrsim 1$ [86]. Thus, for typical values of Love numbers $k_2 \lesssim 10^{-1}$, it is more likely to observe resonances for moderate to extreme mass-ratio binaries $10^{-3} \leqslant q \leqslant 10^{-5}$.

We can also express k_2 in terms of the frequency $\omega_{12} \equiv \omega_2$ of the $n=1$, $l=2$ mode. At resonance, from equation (6), $Q \sim \Delta E^{\rm int}$, where $\Delta E^{\rm int} = \frac{1}{2}M\omega_2^2 R^2$ is the energy of the oscillating star at resonance. Thus, on dimensional grounds, we get $Q \sim \Delta E^{\rm int} R^2$. For example, for a constant energy density perturbation $Q = \frac{3}{5}\Delta E^{\rm int} R^2$, while typical non-constant energy density profiles result in a numerical prefactor $\lesssim 1$ [61] (see also [29]). During resonance, the typical frequency of excitation $\omega \approx \sqrt{M/b^3}$, where $b \gg R$ is the orbital separation distance. Thus, the internal energy of excitation constitutes a fraction of the UCO typical energy $M\omega^2 R^2 \approx MR^3/b^3 \ll M$.

Substituting the expressions for Q and $\Delta E^{\rm int}$, we arrive at our final result for the Love number

$$k_2 \simeq \mathcal{N}\omega_2^2 R^2 \,, \tag{20}$$

where $\mathcal{N}$ is an order unity dimensionless number that depends on the object's energy density profile and contains the numerical factors in the definition of the Love number [29]. We will use equation (20) to determine the detectability of k_2 in the next section.

Remarkably, in [29], it is shown that the gravitational polarizability of objects which possess a discrete spectrum of quantum mechanical energy levels is similar to that of classical stars. This follows from the fact that the wavelength of the oscillation is of order of the star radius. We shall refer these objects as 'quantum black holes' (QBHs) to mean the quantum state that corresponds to a classical BH. The idea is justified on the grounds of the Bohr correspondence principle, where at macroscopic excitations, expectation values are replaced by classical observables. Therefore, an excited quantum macroscopic object can be treated as a semi-classical oscillating fluid-like object that satisfy equation (4). Using standard time-independent quantum perturbation theory, the Love number of QBHs is given by [29, 30]

$$k_2 \simeq \frac{3}{4R^5}\frac{|\langle\Psi_0|\hat{Q}|n=1,l=2\rangle|^2}{\Delta E_1^{\rm int}} \,. \tag{21}$$

where Ψ_0 is the QBH ground state, $\hat{Q}$ is the mass moment operator that obeys the no-hair theorem; $\langle\Psi_0|\hat{Q}|\Psi_0\rangle = 0$. The definition of equation (17) is restored by applying the Bohr correspondence principle and replacing expectations values with classical observables, $\langle\Psi_0|\hat{Q}|n,l=2\rangle \leftrightarrow Q_n$. In this form, equation (21) can be treated in a similar way to the classical treatment of equations (17) and (20), which eventually recovers the result $k_2 \simeq \mathcal{N}\omega_2^2 R^2$. The result is valid for any object of radius R, quantum or classical, which has a quadrupole internal mode whose nonrelativistic frequency is ω_2.

4. Detectability

In this section, using the Fisher method, we give a quantitative estimation of the statistical error in measuring the Love number. We discuss the prospects for detection of a non-vanishing Love number with the future space LISA detector and demonstrate that during the inspiral, it is more likely to detect the Love number with resonances rather than tidal deformability. We would like to stress that the results of our statistical analysis should be viewed as a preliminary evaluation of the detection prospects, indicating that it is indeed worthwhile to perform a more accurate analysis.

We evaluate the detectability of the Love numbers through resonant excitations with the planned space telescope LISA, which according to [9], could track and observe moderate to extreme mass-ratio binaries from the early stages of the inspiral and up to the merger with high

SNR. Before addressing the precise statistical analysis, we wish to emphasize that for most of the range of the binary masses and spins and for Love numbers $k_2 \lesssim 10^{-1}$, the leading order 2.5PN resonance phase term is comparable to the other effects entering at 2.5PN, such as the PP 2.5PN term and the leading order tidal heating term. For smaller values of q, the resonance phase term becomes significant. Since it is established that LISA can detect the other 2.5PN effects, we expect that LISA could be able to detect the Love numbers with high confidence.

To evaluate the statistical error, we employ the Fisher information method. Assuming a signal $s(t) = h(t,\theta^i) + n$, with the uncorrelated noise n, a model signal $h(t,\theta^i)$ with model parameters θ^i. For high SNR events, the posterior distribution takes the form

$$p\left(\theta^i|s\right) \propto \mathrm{e}^{-\frac{1}{2}\Delta\theta^i\,\Delta\theta^j\Gamma_{ij}}\,. \tag{22}$$

where Γ_{ij} is the Fisher matrix defined as

$$\Gamma_{ij} = \left(\frac{\partial h}{\partial\theta^i}\middle|\frac{\partial h}{\partial\theta^j}\right)\,. \tag{23}$$

With the inner product defined by $(h_1|h_2) = 4\mathrm{Re}\int_{f_{\min}}^{f_{\max}}\frac{\tilde{h}_1(f)\tilde{h}_2^*(f)}{S_n(f)}\mathrm{d}f$, and $S_n(f)$ is LISA's design noise spectral density. The model parameters are $\theta^i = (\ln\mathcal{A}, \ln\mathcal{M}_c, \eta, \Phi_c, t_c, \chi_1, \chi_2, k_2)$, where $\mathcal{A}$ is the amplitude, $\mathcal{M}_c$ is the chirp mass, η is the symmetric mass-ratio, Φ_c and t_c are the phase and time at coalescence, χ_i are the companions spin parameter and k_2 is the Love number given in equation (20). The statistical error in measuring k_2 is related to the Fisher matrix,

$$\sigma_{k_2} = \sqrt{\langle\Delta k_2\rangle^2} = \sqrt{(\Gamma^{-1})_{k_2k_2}}. \tag{24}$$

We consider quasi-circular orbits and employ the analytical frequency domain post-Newtonian approximation TaylorF2 [87–89]. The frequency domain GW waveform describing the binary inspiral is of the form $\tilde{h}(f,\theta_i) = \mathcal{A}\mathrm{e}^{\mathrm{i}\Phi}$, where Φ is the phase evolution in equation (2). From equation (20), for $q \ll 1$, the instantaneous phase shift at resonance becomes

$$\Delta\Phi_{\mathrm{Res}} \approx \mathcal{N}\,\frac{\omega_2^2R^2}{20q}. \tag{25}$$

In our analysis we included correction terms up to 3PN order and neglected the higher order tidal deformability terms that depend on the Love number and enter at 5PN and 6PN order (see section 4.1).

Additionally, since our model is valid only until the ISCO, the frequency range $\omega_2 > 0.75\omega_{\mathrm{ISCO}}$ is not included in our analysis. Consequently, it is beneficial to parameterize the oscillation frequencies in terms of the ISCO frequency $\omega_2 = \alpha\omega_{\mathrm{ISCO}}$, where $0 < \alpha \leqslant 1$, and $\omega_{\mathrm{ISCO}}(\chi)$ is spin-dependent. This also means that resonance at the ISCO sets the maximal value of the Love number that can be detected $k_2^{\max} = \mathcal{N}\omega_{\mathrm{ISCO}}^2R^2$.

Since PN based templates are more accurate for comparable mass ratio inspirals and less accurate for EMRIs. We wish to justify their implementation in current analysis. The application of the PN templates for EMRIs and IMRIs was studied in [90–92], their results describe well slowly spinning compact objects, as we do in the current analysis [91]. They calculate the accumulated phase error in using PN waveforms compared to full NR simulations and demonstrate that 5.5PN results in a relative phase error of $0.1 \lesssim \Delta\Phi_{\mathrm{error}} \lesssim 10$ for a mass ratio of $q = 10^{-4}$ and a six months observation where the lower (upper) bound corresponds to observation in the early (late) inspiral. The error increases towards the ISCO, and it is less significant in the early inspiral where the orbital velocities are small.

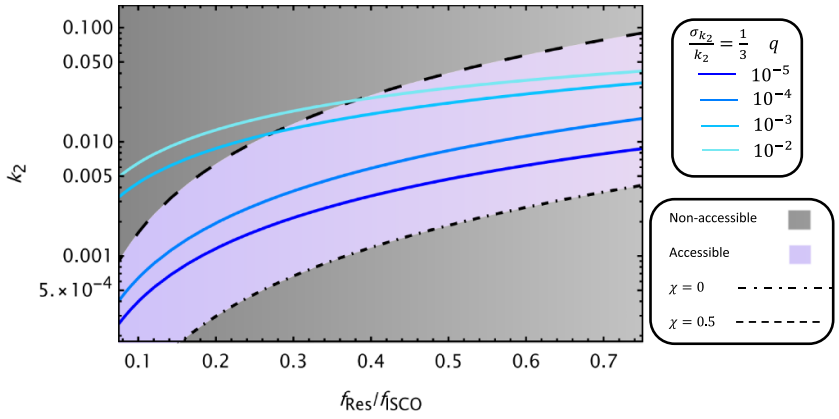

Figure 1. The solid blue lines correspond to a potential measurement of k_2 for a given mass ratio q, with relative error $\sigma_{k_2}/k_2 = 1/3$. The region above each solid line corresponds potential measurement of k_2 with a relative error smaller than $1/3$. As anticipated by equation (18), for a smaller mass ratio, the error on measuring a specific k_2 is smaller and it is possible to measure smaller values of k_2. The purple region describes the parameter space accessible to our model for values of the spin parameter between 0 and 0.5, taking into account Love-resonance-spin relation: $k_2 \propto \omega_{\rm ISCO}(\chi)R(\chi)$, such that a given Love number corresponds to a specific resonance frequency and spin parameter. The grey region describes the parameter space which is not accessible to our model for these values of the spin parameters.

To understand the effect of the phase error when using the PN waveforms, note that the leading 2.5PN resonance phase is $\Delta\Phi_{\rm Res} \sim 1/q$. Thus, for EMRIs, $\Delta\Phi_{\rm Res} \gg \Delta\Phi_{\rm error}$, which particular holds away from the ISCO. Consequently, due to the large resonance dephasing, the effect of omitting the higher order correction terms in the PN expansion would not be significant for the evaluation of resonances. Especially for high SNR events, which according to LISA could be observed under some favorable conditions with SNR ~ 100 [93, 94]. The threshold phase error required for detection $\Delta\Phi^{\rm min}_{\rm Res} \sim 1/{\rm SNR}$, so resonances are already distinguished at dephasing of 10 milliradians.

To improve the accuracy of the results and to avoid the significant phase error accumulated towards the ISCO, we restricted the analysis to the early inspiral part where the resulting error due to omitting the higher order terms is negligible. From the frequency range of the various events we consider $f_{\rm max} = [3.5, 5.5] \times 10^{-3}$Hz and $f_{\rm min}$ is chosen to guarantee an observation time of $\Delta T_{\rm obs} \lesssim 6$ months. Since the error reduces when reducing the binary mass-ratio, we consider intermediate as well as extreme mass-ratio binaries with $q = [10^{-2}, 10^{-3}, 10^{-4}, 10^{-5}]$, where the central object mass is $M_1 = 10^6 M_\odot$, and small to moderate Kerr spin parameters $\chi^i = [0, 0.1, 0.2, 0.3, 0.4, 0.5]$, at a typical luminosity distance $D_l = 2$Gpc. We also average over the sky location parameters [89]. We assume equal spins $\chi_1 = \chi_2$ that are aligned with the orbital angular velocity vector. For the model-dependent order unity coefficient $\mathcal{N}$, we use the estimation derived in [29], and consider $\mathcal{N} \in [0.1, 1]$.

In figure 1, the purple region shows the analytical Love-resonance-spin relation described in equation (20) that is determined by our model, where a given Love number corresponds to a specific resonance frequency and a spin parameter. This region describes the parameter space accessible to our model and is independent of the detector properties. In our analysis, the largest accessible k_2 is reached for $\mathcal{N} = 1$, $\alpha = 1$ and $\chi = 0.5$, resulting in $k_2^{\rm max} \approx 0.159$,

larger values are inaccessible to our model. The grey region is the parameter space region that our model cannot describe.

For the completeness of our model and the detection analysis, we wish to estimate the impact of the gravitational tidal force exerted by the lighter companion on the primary, and evaluate the distance at which the force applied on a fluid element at the surface of the primary exceeds its gravitational pull, $(M_2/b^3)R_2 = M_1/R_1^2$, which leads to a distance $b = (qR_2R_1^2)^{1/3} \sim q^{2/3}R_1 \ll R_{\rm ISCO}$. Since $q \ll 1$, the fluid does not experience significant changes due to companion tidal forces, and the analysis holds until the ISCO.

4.1. Comparison to Tidal-deformability

We now turn to estimate the relative magnitude of the resonance phase shift effects compared to the magnitude of tidal deformation effects on the phase evolution. When estimating these effects we ignore the possibility of resonant excitation. Furthermore, we focus on the adiabatic regime during the inspiral and far enough from the merger. In this regime, static tides are more important than dynamical tides [46, 60]. As shown there, dynamical tides become important at higher orbital velocities and particularly before the merger (after the ISCO). These scenarios are particularly relevant for binaries where the primary is a neutron star whose internal spectrum contains high-frequency modes. However, here we considered different scenarios where resonances occur during the inspiral at low orbital velocities.

To leading PN order, the tidal deformability contribution to the phase for $q \ll 1$ takes the form $\Phi_{\rm TD}(f) \sim k_2 v^5/q$, where $v = (\pi M f)^{1/3}$ is the orbital velocity. The accumulated phase throughout the inspiral is given by

$$\Delta\Phi_{\rm TD} = \int_{f_{\rm min}}^{f_{\rm ISCO}} f \frac{{\rm d}^2\Phi_{\rm TD}(f)}{{\rm d}f^2}{\rm d}f \sim \frac{k_2}{q} v_{\rm ISCO}^5 \,. \tag{26}$$

For a case for which the central object mass is $M_1 = 10^6 M_\odot$ and for small to moderate spin parameters, we find $v_{\rm ISCO}^5 \sim 0.01$. Comparing to the instantaneous resonance phase jump equation (12), $\Delta\Phi_{\rm TD}/\Delta\Phi_{\rm Res} \sim v_{\rm ISCO}^5$. Therefore, we would expect to have a larger error in the measurement of the Love number relying on tidal deformability.

We calculated the statistical error in measuring the Love number through tidal deformability and compared it to a measurement via resonance effects and found that the previous estimate is indeed correct. We repeated the statistical evaluation performed above, excluding resonance effects and including the leading tidal deformation terms entering the phase at 5PN and 6PN order [35, 95, 96]. Our estimates are comparable to previous estimates, for example, [36, 37] in the range that we can compare them.

The results of the calculation of the ratio of the relative errors in measuring the Love numbers, denoted by $\sigma_{k_2}^{\rm Res}/\sigma_{k_2}^{\rm TD}$ for different spin parameters $0 \leqslant \chi \leqslant 0.5$ are presented in figure 2.

5. Summary and conclusion

The future measurement of GWs produced during BBH inspirals by the planned GW detector LISA will present an unprecedented opportunity to test GR. Hypothetical tidal interactions between the inspiraling objects would affect the waveform of the emitted GWs in a way that could only be possible if astrophysical BHs were actually UCOs possessing an internal structure rather than the structureless objects predicted by GR.

We discussed how the resonant excitation of the hypothetical nonrelativistic interior modes of astrophysical BHs changes the phase of the emitted GW waveform when compared to the

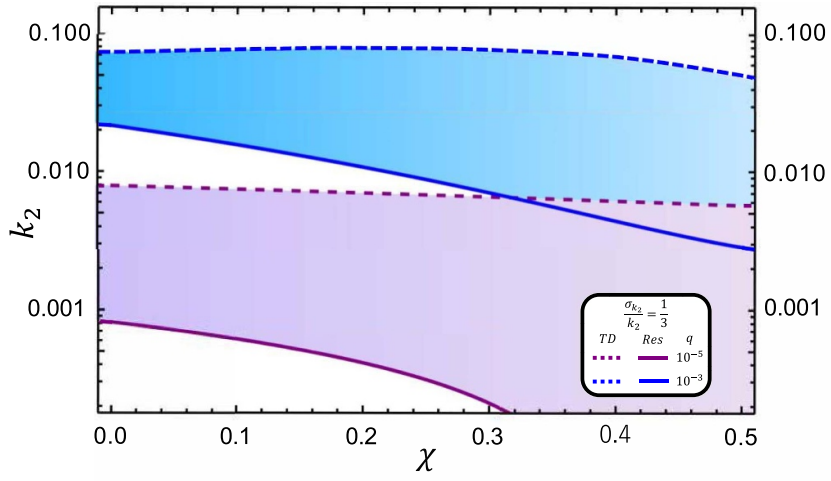

Figure 2. The figure displays the relative statistical errors in measuring k_2 with resonance excitations and tidal deformation. For a given k_2 and χ we calculate $\sigma_{k_2}^{\rm res}$ without tidal deformation effects and $\sigma_{k_2}^{\rm TD}$ without resonances. The results show a preference for detecting k_2 with resonance effects. The preference is more apparent for a smaller mass ratio q. The colored regions enclosed by the solid and the dashed lines mark the additional parameter space that resonances can probe compared to tidal deformation.

phase predicted by GR. The nonrelativistic nature of the modes was crucial to the possibility of resonantly exciting them, because in this case they could be excited when the two objects are still far apart. In this case, the resonance occurs a long time before the ISCO is reached and leads to a significant dephasing. We find that regardless the specific details of the primary's interior composition, the phase shift is governed by a single intrinsic quantity—the dimensionless tidal Love number k_2.

We performed a preliminary evaluation of the statistical error in measuring the Love number k_2 by LISA using the resonance effect. We concluded that the smallness of the resulting statistical error indicates that k_2 could actually be detected by LISA with impressive accuracy by observing intermediate and extreme mass-ratio inspirals and that, therefore, it is worthwhile to perform a more accurate analysis. Additionally, currently, there do not exist precise population estimation for EMRIs, and their formation channels is an open question that depends on complex astrophysical factors [97, 98]. However, these binaries are considered as a possible source for GW emission which are expected to be observed by LISA [9, 10]. Accordingly, the values chosen for the primary mass and the luminosity distance are considered as a typical choices that covers various formation channels of EMRIs and IMRIs [97, 98]

We further compared the statistical error for detection of the Love number relying on tidal deformation effects with the error when using resonance effects and concluded that prospects of measuring k_2 using resonance effects are much better. The results reveal additional sensitivity-enhancement factors whose origin is the Love-resonance-spin relation. First, the statistical error in measuring the Love number reduces for BHs with higher spin, because for such BHs, the inspiral duration is longer. Second, the statistical error in measuring the Love number reduces if the inspiral includes a range of higher orbital velocities, which could lead to excitation of higher internal frequencies, which, in turn, correspond to the BH having a larger Love number.

Our conclusion is that the effects of resonant excitation of astrophysical BHs during intermediate and extreme mass-ratio inspirals provide the best opportunity for putting bounds on, or detecting, the tidal Love number of astrophysical BHs and thus providing evidence of physics beyond GR. Nevertheless, we stress that the results of our statistical analysis should be viewed as preliminary estimates for the detection prospects. A comprehensive statistical treatment requires more accurate waveform modelling and should consider LISA's ability to track and discriminate several EMRIs simultaneously [9] or other sources of degeneracy, such as the effects of near by objects.

Our analysis is based on a general theoretical framework which only requires the existence of a set of nonrelativistic internal modes and does not require specifying the detailed properties of the central object. The entire dependence on the interior composition is parameterized in terms of the dimensionless tidal Love numbers. Our results could therefore potentially be applied to other models of ultra-compact BH mimickers if they possess a similar spectrum.

Data availability statement

All data that support the findings of this study are included within the article (and any supplementary files).

Acknowledgments

We thank Vitor Cardoso, Tanja Hinderer and Ely Kovetz for useful discussions. The research is supported by the German Research Foundation through a German-Israeli Project Cooperation (DIP) grant 'Holography and the Swampland' and by VATAT (Israel planning and budgeting committee) grant for supporting theoretical high energy physics. The research of Y S is supported by a Minerva Fellowship of the Minerva Stiftung Gesellschaft fuer die Forschung mbH.

Appendix

A.1. The effect of viscosity

The reason for neglecting the dissipation term is because the dimensionless coefficient γ is determined by the viscosity of the interior matter and leads to viscous dissipation. This effect was found in [99] (see also [44, 84]) to be negligible for all physical matter configurations and therefore is irrelevant for the dynamics of modes resonance. Moreover, we are interested in the resonance dephasing that is determined by the total energy absorbed into a single mode, equation (9). This is a known situation for damped driven oscillators equation (4), where the total energy that excites the mode is determined by the external force as we show below.

Following [45], since $\gamma_n \ll \omega_n$, the amplitude can be written as

$$a_{nlm} = \tilde{a}_{nlm} \mathrm{e}^{-\mathrm{i}\omega_n t}. \tag{27}$$

Taking a second order time derivative

$$\dot{a}_{nlm} = \left(\dot{\tilde{a}}_{nlm} - i\omega_n \tilde{a}_{nlm}\right) \mathrm{e}^{-\mathrm{i}\omega_n t}, \tag{28}$$

$$\ddot{a}_{nlm} = \left(\ddot{\tilde{a}}_{nlm} - 2i\omega_n \dot{\tilde{a}}_{nlm} - \omega_n^2 \tilde{a}_{nlm}\right) \mathrm{e}^{-\mathrm{i}\omega_n t}, \tag{29}$$

then equation (4) becomes

$$\ddot{\tilde{a}}_{nlm} + 2(\gamma_n - i\omega_n)\dot{\tilde{a}}_{nlm} = \mathcal{F}(t)_{nlm} e^{-im\phi(t))}. \tag{30}$$

And again neglecting the damping rate compared to the mode frequency.

Integration over time interval $[t_1, t_2]$ around resonance, assuming that the resonance effect is significant enough. Neglecting the rates of change before and after the resonance

$$\int_{t_1}^{t_2} \ddot{\tilde{a}}_{nlm} dt = \left[\dot{\tilde{a}}_{nlm}(t_2) - \dot{\tilde{a}}_{nlm}(t_1)\right] = 0, \tag{31}$$

and assuming a significant growth of the amplitude

$$\int_{t_1}^{t_2} \dot{\tilde{a}}_{nlm} dt = \tilde{a}_{nlm}(t_2). \tag{32}$$

For the RHS, we expand the interval to regions where the exponent oscillates fast enough. Therefore those regions add zero contribution to the integral

$$\int_{t_1}^{t_2} \mathcal{N}_{lm} \frac{\mathcal{E}_l Q_{nl}}{MR^2} e^{i\omega_n t - im\phi(t)} dt \approx \int_{\infty}^{-\infty} \mathcal{N}_{lm} \frac{\mathcal{E}_l Q_{nl}}{MR^2} e^{i\omega_n t - im\phi(t)} dt. \tag{33}$$

The resonance condition is given by

$$|m|\dot{\phi}_R = \omega_n. \tag{34}$$

Using the stationary phase approximation, we find that the amplitude of the oscillator after resonance is given by

$$a_{nlm} = \sqrt{\frac{\pi}{m\ddot{\phi}_R}} \frac{\mathcal{F}_{R,nlm} e^{-im\phi_R}}{\omega_n} i e^{-i\omega_n t}. \tag{35}$$

Which recovers equation (7) when taking the time to be the time at resonance and neglecting the damping rate.

ORCID iD

Yotam Sherf https://orcid.org/0000-0003-4687-5454

References

[1] Bekenstein J D 1972 Nonexistence of baryon number for static black holes *Phys. Rev.* D **5** 1239–46
[2] Abbott B P *et al* (LIGO Scientific and Virgo) 2016 Observation of gravitational waves from a binary black hole merger *Phys. Rev. Lett.* **116** 061102
[3] Flanagan E E and Hinderer T 2008 Constraining neutron star tidal Love numbers with gravitational wave detectors *Phys. Rev.* D **77** 021502
[4] Hinderer T, Lackey B D, Lang R N and Read J S 2010 Tidal deformability of neutron stars with realistic equations of state and their gravitational wave signatures in binary inspiral *Phys. Rev.* D **81** 123016
[5] De S, Finstad D, Lattimer J M, Brown D A, Berger E and Biwer C M 2018 Tidal deformabilities and radii of neutron stars from the observation of GW170817 *Phys. Rev. Lett.* **121** 091102
De S, Finstad D, Lattimer J M, Brown D A, Berger E and Biwer C M 2018 *Phys. Rev. Lett.* **121** 259902 (erratum)

[6] Maselli A, Cardoso V, Ferrari V, Gualtieri L and Pani P 2013 equation-of-state-independent relations in neutron stars *Phys. Rev.* D **88** 023007
[7] Yazadjiev S S, Doneva D D and Kokkotas K D 2018 Tidal Love numbers of neutron stars in $f(R)$ gravity *Eur. Phys. J.* C **78** 818
[8] Pacilio C, Maselli A, Fasano M and Pani P 2022 Ranking love numbers for the neutron star equation of state: the need for third-generation detectors *Phys. Rev. Lett.* **128** 101101
[9] Amaro-Seoane P *et al* 2017 Laser interferometer space antenna (arXiv:1702.00786 [astro-ph.IM])
[10] Arun K G *et al* (LISA) 2022 New horizons for fundamental physics with LISA *Living Rev. Relativ.* **25** 4
[11] Penrose R 1965 Gravitational collapse and space-time singularities *Phys. Rev. Lett.* **14** 57
[12] Hawking S W and Penrose R 1970 The singularities of gravitational collapse and cosmology *Proc. R. Soc.* A **314** 529
[13] Buchdahl H 1959 General relativistic fluid spheres *Phys. Rev.* **116** 1027
[14] Chandrasekhar S 1964 Dynamical instability of gaseous masses approaching the schwarzschild limit in general relativity *Phys. Rev. Lett.* **12** 114
[15] Chandrasekhar S 1964 The dynamical instability of gaseous masses approaching the schwarzschild limit in general relativity *Astrophys. J.* **140** 417
[16] Bondi H 1964 Massive spheres in general relativity *Proc. R. Soc.* A **282** 303
[17] Brustein R and Medved A J M 2019 Resisting collapse: how matter inside a black hole can withstand gravity *Phys. Rev.* D **99** 064019
[18] Frolov V P and Zelnikov A 2017 Quantum radiation from an evaporating nonsingular black hole *Phys. Rev.* D **95** 124028
[19] Carballo-Rubio R, Di Filippo F, Liberati S, Pacilio C and Visser M 2018 On the viability of regular black holes *J. High Energy Phys.* JHEP07(2018)023
[20] Damour T and Nagar A 2009 Relativistic tidal properties of neutron stars *Phys. Rev.* D **80** 084035
[21] Binnington T and Poisson E 2009 Relativistic theory of tidal Love numbers *Phys. Rev.* D **80** 084018
[22] Chia H S 2021 Tidal deformation and dissipation of rotating black holes *Phys. Rev.* D **104** 024013
[23] Charalambous P, Dubovsky S and Ivanov M M 2021 Hidden symmetry of vanishing love numbers *Phys. Rev. Lett.* **127** 101101
[24] Charalambous P, Dubovsky S and Ivanov M M 2021 On the vanishing of love numbers for Kerr black holes *J. High Energy Phys.* JHEP05(2021)038
[25] Hui L, Joyce A, Penco R, Santoni L and Solomon A R 2022 Ladder symmetries of black holes. Implications for love numbers and no-hair theorems *J. Cosmol. Astropart. Phys.* JCAP01(2022)032
[26] Ben Achour J, Livine E R, Mukohyama S and Uzan J-P 2022 Hidden symmetry of the static response of black holes: applications to Love numbers *J. High Energy Phys.* JHEP07(2022)112
[27] Maselli A, Pani P, Cardoso V, Abdelsalhin T, Gualtieri L and Ferrari V 2018 Probing Planckian corrections at the horizon scale with LISA binaries *Phys. Rev. Lett.* **120** 081101
[28] Cardoso V, Franzin E, Maselli A, Pani P and Raposo G 2017 Testing strong-field gravity with tidal Love numbers *Phys. Rev.* D **95** 084014
[29] Brustein R and Sherf Y 2022 Quantum love numbers *Phys. Rev.* D **105** 024043
[30] Brustein R and Sherf Y 2022 Classical love number for quantum black holes *Phys. Rev.* D **105** 024044
[31] Brustein R and Sherf Y 2021 Tidal deformation of quantum black holes *Int. J. Mod. Phys.* D **30** 2142011
[32] Datta S 2022 Probing horizon scale quantum effects with Love *Class. Quantum Grav.* **39** 225016
[33] Damour T, Nagar A and Villain L 2012 Measurability of the tidal polarizability of neutron stars in late-inspiral gravitational-wave signals *Phys. Rev.* D **85** 123007
[34] Abbott B P *et al* (LIGO Scientific and Virgo) 2017 GW170817: observation of gravitational waves from a binary neutron star inspiral *Phys. Rev. Lett.* **119** 161101
[35] Sennett N, Hinderer T, Steinhoff J, Buonanno A and Ossokine S 2017 Distinguishing boson stars from black holes and neutron stars from tidal interactions in inspiraling binary systems *Phys. Rev.* D **96** 024002
[36] Piovano G A, Maselli A and Pani P 2023 Constraining the tidal deformability of supermassive objects with extreme mass ratio inspirals and semianalytical frequency-domain waveforms *Phys. Rev.* D **107** 024021
[37] Zi T and Li P-C 2023 Probing the tidal deformability of the central object with analytic kludge waveforms of an extreme-mass-ratio inspiral *Phys. Rev.* D **108** 024018

[38] Cowling T G and Phil M A D 1941 *Mon. Not. R. Astron. Soc.* **101** 367–75
[39] Lai D 1994 Resonant oscillations and tidal heating in coalescing binary neutron stars *Mon. Not. R. Astron. Soc.* **270** 611
[40] Reisenegger A and Goldreich P 1994 Excitation of neutron star normal modes during binary inspiral *Astrophys. J.* **426** 68
[41] Shibata M 1994 Effects of tidal resonances in coalescing compact binary systems *Prog. Theor. Phys.* **91** 871–83
[42] Kokkotas K D and Schaefer G 1995 Tidal and tidal resonant effects in coalescing binaries *Mon. Not. R. Astron. Soc.* **275** 301
[43] Ho W C G and Lai D 1999 Resonant tidal excitations of rotating neutron stars in coalescing binaries *Mon. Not. R. Astron. Soc.* **308** 153
[44] Flanagan E E and Racine E 2007 Gravitomagnetic resonant excitation of Rossby modes in coalescing neutron star binaries *Phys. Rev.* D **75** 044001
[45] Lai D and Wu Y 2006 Resonant tidal excitations of inertial modes in coalescing neutron star binaries *Phys. Rev.* D **74** 024007
[46] Hinderer T *et al* 2016 Effects of neutron-star dynamic tides on gravitational waveforms within the effective-one-body approach *Phys. Rev. Lett.* **116** 181101
[47] Yu H and Weinberg N N 2017 Resonant tidal excitation of superfluid neutron stars in coalescing binaries *Mon. Not. R. Astron. Soc.* **464** 2622–37
[48] Xu W and Lai D 2017 Resonant tidal excitation of oscillation modes in merging binary neutron stars: inertial-gravity modes *Phys. Rev.* D **96** 083005
[49] Yang H 2019 Inspiralling eccentric binary neutron stars: orbital motion and tidal resonance *Phys. Rev.* D **100** 064023
[50] Pratten G, Schmidt P and Hinderer T 2020 Gravitational-wave asteroseismology with fundamental modes from compact binary inspirals *Nat. Commun.* **11** 2553
[51] Poisson E 2020 Gravitomagnetic tidal resonance in neutron-star binary inspirals *Phys. Rev.* D **101** 104028
[52] Pnigouras P, Gittins F, Nanda A, Andersson N and Jones D I 2022 Rotating love: the dynamical tides of spinning Newtonian stars (arXiv:2205.07577 [gr-qc])
[53] Gamba R and Bernuzzi S 2023 Resonant tides in binary neutron star mergers: analytical-numerical relativity study *Phys. Rev.* D **107** 044014
[54] Berry C P L, Cole R H, Cañizares P and Gair J R 2016 Importance of transient resonances in extreme-mass-ratio inspirals *Phys. Rev.* D **94** 124042
[55] Bonga B, Yang H and Hughes S A 2019 Tidal resonance in extreme mass-ratio inspirals *Phys. Rev. Lett.* **123** 101103
[56] Gupta P, Bonga B, Chua A J K and Tanaka T 2021 Importance of tidal resonances in extreme-mass-ratio inspirals *Phys. Rev.* D **104** 044056
[57] Gupta P, Speri L, Bonga B, Chua A J K and Tanaka T 2022 Modeling transient resonances in extreme-mass-ratio inspirals *Phys. Rev.* D **106** 104001
[58] Chakrabarti S, Delsate T and Steinhoff J 2013 New perspectives on neutron star and black hole spectroscopy and dynamic tides (arXiv:1304.2228 [gr-qc])
[59] Chakrabarti S, Delsate T and Steinhoff J 2013 Effective action and linear response of compact objects in Newtonian gravity *Phys. Rev.* D **88** 084038
[60] Steinhoff J, Hinderer T, Buonanno A and Taracchini A 2016 Dynamical tides in general relativity: effective action and effective-one-body Hamiltonian *Phys. Rev.* D **94** 104028
[61] Andersson N and Pnigouras P 2020 Exploring the effective tidal deformability of neutron stars *Phys. Rev.* D **101** 083001
[62] Gupta P K, Puecher A, Pang P T H, Janquart J, Koekoek G and Broeck Van Den C 2022 Determining the equation of state of neutron stars with Einstein Telescope using tidal effects and r-mode excitations from a population of binary inspirals (arXiv:2205.01182 [gr-qc])
[63] Gupta P K, Steinhoff J and Hinderer T 2023 Effect of dynamical gravitomagnetic tides on measurability of tidal parameters for binary neutron stars using gravitational waves (arXiv:2302.11274 [gr-qc])
[64] Cardoso V, del Rio A and Kimura M 2019 Distinguishing black holes from horizonless objects through the excitation of resonances during inspiral *Phys. Rev.* D **100** 084046
Cardoso V, del Rio A and Kimura M 2020 *Phys. Rev.* D **101** 069902 (erratum)
[65] Asali Y, Pang P T H, Samajdar A and Van Den Broeck C 2020 Probing resonant excitations in exotic compact objects via gravitational waves *Phys. Rev.* D **102** 024016

[66] Fransen K, Koekoek G, Tielemans R and Vercnocke B 2021 *Phys. Rev.* D **104** 044044
[67] Maggio E, van de Meent M and Pani P 2021 Extreme mass-ratio inspirals around a spinning horizonless compact object *Phys. Rev.* D **104** 104026
[68] Brustein R, Medved A J M and Yagi K 2017 When black holes collide: probing the interior composition by the spectrum of ringdown modes and emitted gravitational waves *Phys. Rev.* D **96** 064033
[69] Brustein R, Medved A J M and Simhon T 2022 Black holes as frozen stars *Phys. Rev.* D **105** 024019
[70] Brustein R, Medved A J M, Shindelman T and Simhon T 2023 Black holes as frozen stars: regular interior geometry (arXiv:2301.09712 [gr-qc])
[71] Brustein R, Medved A J M and Shindelman T 2023 Defrosting frozen stars: spectrum of internal fluid modes (arXiv:2304.04984 [gr-qc])
[72] Robson T, Cornish N J and Liu C 2019 The construction and use of LISA sensitivity curves *Class. Quantum Grav.* **36** 105011
[73] Bekenstein J D and Mukhanov V F 1995 Spectroscopy of the quantum black hole *Phys. Lett.* B **360** 7–12
[74] Bekenstein J D 1997 Quantum black holes as atoms (arXiv:gr-qc/9710076 [gr-qc])
[75] Mathur S D 2005 The fuzzball proposal for black holes: an elementary review *Fortsch. Phys.* **53** 793–827
[76] Guo B, Hampton S and Mathur S D 2018 Can we observe fuzzballs or firewalls? *J. High Energy Phys.* JHEP07(2018)162
[77] Brustein R and Medved A J M 2018 Quantum hair of black holes out of equilibrium *Phys. Rev.* D **97** 044035
[78] Brustein R and Medved A J M 2017 Black holes as collapsed polymers *Fortsch. Phys.* **65** 1600114
[79] Brustein R and Medved A J M 2017 Emergent horizon, Hawking radiation and chaos in the collapsed polymer model of a black hole *Fortsch. Phys.* **65** 1600116
[80] Brustein R, Medved A J M and Shindelman T 2023 Defrosting frozen stars: spectrum of internal fluid modes *Phys. Rev.* D **108** 044058
[81] Letelier P S 1979 Clouds of strings in general relativity *Phys. Rev.* D **20** 1294–302
[82] Press W H and Teukolsky S A 1977 On formation of close binaries by two-body tidal capture *Astrophys. J.* **213** 183
[83] Poisson E 2009 Tidal interaction of black holes and Newtonian viscous bodies *Phys. Rev.* D **80** 064029
[84] Sherf Y 2021 Tidal-heating and viscous dissipation correspondence in black holes and viscous compact objects *Phys. Rev.* D **103** 104003
[85] Thorne K S, Price R H and Macdonald D A 1986 *Black Holes: The Membrane Paradigm* (Yale University Press)
[86] Lindblom L, Owen B J and Brown D A 2008 Model waveform accuracy standards for gravitational wave data analysis *Phys. Rev.* D **78** 124020
[87] Damour T, Iyer B R and Sathyaprakash B S 2001 A comparison of search templates for gravitational waves from binary inspiral *Phys. Rev.* D **63** 044023
Damour T, Iyer B R and Sathyaprakash B S 2005 *Phys. Rev.* D **72** 029902 (erratum)
[88] Arun K G, Iyer B R, Sathyaprakash B S and Sundararajan P A 2005 Parameter estimation of inspiralling compact binaries using 3.5 post-Newtonian gravitational wave phasing: the Non-spinning case *Phys. Rev.* D **71** 084008
Arun K G, Iyer B R, Sathyaprakash B S and Sundararajan P A 2005 *Phys. Rev.* D **72** 069903 (erratum)
[89] Buonanno A, Iyer B, Ochsner E, Pan Y and Sathyaprakash B S 2009 Comparison of post-Newtonian templates for compact binary inspiral signals in gravitational-wave detectors *Phys. Rev.* D **80** 084043
[90] Fujita R 2012 Gravitational radiation for extreme mass ratio inspirals to the 14th post-Newtonian order *Prog. Theor. Phys.* **127** 583–90
[91] Fujita R 2012 Gravitational waves from a particle in circular orbits around a schwarzschild black hole to the 22nd post-Newtonian order *Prog. Theor. Phys.* **128** 971–92
[92] Varma V, Fujita R, Choudhary A and Iyer B R 2013 Comparison of post-Newtonian templates for extreme mass ratio inspirals *Phys. Rev.* D **88** 024038
[93] Amaro-Seoane P, Gair J R, Freitag M, Coleman Miller M, Mandel I, Cutler C J and Babak S 2007 Astrophysics, detection and science applications of intermediate- and extreme mass-ratio inspirals *Class. Quantum Grav.* **24** R113–69
[94] Amaro-Seoane P *et al* 2017 Laser interferometer space antenna (arXiv:1702.00786 [astroph.IM])

[95] Bini D, Damour T and Faye G 2012 Effective action approach to higher-order relativistic tidal interactions in binary systems and their effective one body description *Phys. Rev.* D **85** 124034
[96] Hotokezaka K, Kyutoku K, Sekiguchi Y-I and Shibata M 2016 Measurability of the tidal deformability by gravitational waves from coalescing binary neutron stars *Phys. Rev.* D **93** 064082
[97] Berry C P L, Hughes S A, Sopuerta C F, Chua A J K, Heffernan A, Holley-Bockelmann K, Mihaylov D P, Miller M C and Sesana A 2019 The unique potential of extreme mass-ratio inspirals for gravitational-wave astronomy (arXiv:1903.03686 [astro-ph.HE])
[98] Portegies Zwart S F and McMillan S L W 2002 The runaway growth of intermediate-mass black holes in dense star clusters *Astrophys. J.* **576** 899–907
[99] Bildsten L and Cutler C 1992 *Astrophys. J.* **400** 175